



Cr-doped U₃Si₂ composite fuels under steam corrosion

Bowen Gong^a, Lu Cai^b, Penghui Lei^a, Kathryn E. Metzger^b, Edward J. Lahoda^b, Frank A. Boylan^b, Kun Yang^a, Jake Fay^a, Jason Harp^c, Jie Lian^{a,*}

^a Department of Mechanical, Aerospace & Nuclear Engineering, Rensselaer Polytechnic Institute, Troy, NY, 12180, United States

^b Westinghouse Electric Company, United States

^c Oak Ridge National Laboratory, United States

ARTICLE INFO

Keywords:

- A. Corrosion resistance
- B. Spark plasma sintering (SPS)
- C. Accident tolerant fuel (ATF)
- D. Cr doped U₃Si₂
- E. Composite fuel
- F. Steam oxidation test

ABSTRACT

Dense Cr-doped U₃Si₂ composite fuels were manufactured by spark plasma sintering, and the effects of Cr addition on mechanical properties and oxidation resistance were investigated. Dynamic oxidation testing by thermogravimetric analysis revealed significantly improved oxidation resistance of U₃Si₂ with minimal doping of 3 wt% Cr. The onset oxidation temperature increased to above 550 °C in air and ~520 °C in steam conditions for the 5 wt% and 10 wt% Cr-doped composites. Steam corrosion testing under 360 °C for 24 hours indicated well-maintained pellet integrity without pulverization for the 10 wt% Cr-doped U₃Si₂ pellet which only showed minor surface oxidation. The first promising results open up the possibility of designing and manufacturing metal additive-doped U₃Si₂ composite fuels with significantly-improved corrosion resistance as a potential candidate for accident tolerant fuels.

1. Introduction

After the Fukushima event [1,2], U₃Si₂ has drawn intense attention as a potential candidate for accident tolerant fuels (ATFs), replacing traditional oxide fuels in advanced light reactor systems to improve their accident tolerance. Numerous studies have been carried out to manufacture U₃Si₂ and characterize their thermomechanical properties, oxidation and corrosion behavior. In general, U₃Si₂ fuels can be fabricated by arc melting combined with vacuum sintering. For example, Harp [3] applied a powder metallurgy process to fabricate dense U₃Si₂ pellets by arc melting of constitute U and Si following by thermal annealing and vacuum sintering. Over 94 % theoretical density (TD) can be achieved for densified U₃Si₂ pellets. However, the sintered fuel pellets are not uniform in microstructure and phase compositions. Multiple impurities such as uraninite C, USi₃, U₅Si₄, etc. and pores can be observed in the sintered pellets [4]. A subsequent characterization on the Idaho National Laboratory (INL)-fabricated U₃Si₂ reported a distorted U₃Si₂ phase showing enlarged lattice parameters from the ideal triuranium disilicide phase. Mohamad [5] and Lopes [6] later reported the synthesis of the monolithic U₃Si₂ using spark plasma sintering (SPS), achieving 96 % TD and >95 % TD, respectively. As compared with UO₂ which can be sintered at 1600 °C for 5 min by SPS sintering [7] or high-pressure sintering (750 MPa) at 600–700 °C [8], the sintering of

U₃Si₂ generally requires lower temperature as a result of the lower melting temperature of U₃Si₂ (1665 °C) than that of UO₂ (2865 °C). In a recent work [9], we reported that a uniform U₃Si₂ pellet could be obtained by SPS sintering at 1000 °C for 5 min. The SPS sintered pellets have a much-improved morphology and uniform microstructure than fuel pellets prepared by arc melting. Composite fuels were also fabricated using SPS to improve fuel properties. For example, Gong et al. [10] incorporated U₃Si₂ with UO₂ to combine their merits from both fuels. It was reported that an improved thermal conductivity comparing to UO₂ and an enhanced mechanical property comparing to U₃Si₂ were achieved.

On thermomechanical properties, White et al. [11] measured thermal diffusivity using laser flash analysis (LFA) from room temperature up to 1773 K and determined that the thermal conductivity of U₃Si₂ ranged from 8.34 to 25.2 W·m⁻¹·K⁻¹. Mohammad [5] and Gong [9] also performed thermal conductivity measurements and obtained comparable results on SPS-densified U₃Si₂ pellets. In general, the thermal conductivity of U₃Si₂ increases with temperature and is considerably higher than that of UO₂ at elevated temperatures. Antonio [12] reported that room-temperature thermal conductivity of U₃Si₂ was controlled by lattice and electronic, while electrons played a dominant role at elevated temperatures. Mechanical properties of U₃Si₂ were measured with Vickers hardness testing [5,9,13], with the microhardness ranging from

* Corresponding author.

E-mail address: lianj@rpi.edu (J. Lian).

6.1 to 7.5 GPa and fracture toughness ranging from 2.8 to 3.3 MPa·m^{1/2}, varying with microstructure, density, and manufacturing process. Compared to the mechanical properties of UO₂ [14], U₃Si₂ has a comparable microhardness and a significantly higher fracture toughness, suggesting that U₃Si₂ may possess a better resistance against crack propagation.

However, the critical factor limiting the application of U₃Si₂ as the leading ATF for practical reactor application is inferior oxidation and corrosion resistance. U₃Si₂ powder was known to easily ignite in ambient atmosphere and can be oxidized instantly in air. For example, Wood et al. reported the oxidation behavior of U₃Si₂ under the air atmosphere from 25 to 1000 °C and found that the oxidation resistance of U₃Si₂ is significantly inferior to UO₂. The oxidation of U₃Si₂ occurred at an onset temperature of 384 °C by dynamic ramp testing using a thermogravimetric analyzer (TGA). U₃Si₂ fuel pellets were also not as stable as UO₂ when exposed to steam. High-temperature steam testing was conducted on U₃Si₂, U₃Si₅, and UO₂ [15]. U₃Si₂ displayed the worst performance and started to pulverize under 400 °C, while the other two can survive and maintain their integrity under 1000 °C. In a subsequent study regarding the behavior of U₃Si₂ in H₂O [16], it was reported that U₃Si₂ would react not only with oxygen but also hydrogen, generating U₃Si₂H_{1.8}. This hydride phase has a low density and tends to rapidly break up the U₃Si₂ matrix, increasing its surface area/volume ratio and finally the rate of reaction. A rapid mass loss occurs for U₃Si₂ about 100 min. in 400 °C steam conditions due to the ejection of U₃Si₂ particles from the TGA balance, indicating intrinsically high kinetics of oxidation and corrosion of U₃Si₂ as a result of the highly exothermic reaction with oxygen and steam.

Alloying with different additives has been proposed to form U₃Si₂ composites in order to improve their oxidation and corrosion resistance. Aluminum doping was applied in order to delay the onset temperature of U₃Si₂ with the expectation of forming Al₂O₃ as a passivation layer [17]. Wood et al. [18] conducted experiments on the steam oxidation of U₃Si₂ alloys with several additives, such as Cr, Al, and Y, prepared by arc melting. No noticeable enhancement in oxidation resistance was observed for the arc-melted U₃Si₂ fuel pellets doped by Cr and Y additives. Highly non-uniform phases were observed in the arc-melted alloys, and the aggregates of alloying elements limit the alloying effects in improving material's oxidation and corrosion resistance. Aluminum addition in the form of a ternary phase U₃Al₂Si₃ improved the onset oxidation temperature above 600 °C; however, the high loading of Al is the fissile element density below that of UO₂, defying the purpose of using U₃Si₂ as a high-density fuel for ATF application.

In this work, we report the design and fabrication of the Cr-doped U₃Si₂ pellets with different dopant amounts, including 3 wt%, 5 wt%, and 10 wt%. The pellets were fabricated by combining high energy ball milling (HEBM) and SPS. Cr was selected as an additive and was expected to form Cr₂O₃ as a protection against further oxidation of the U₃Si₂ matrix. Therefore, a microstructure with a uniform distribution of the Cr additives through the U₃Si₂ matrix will be necessary in order to form the oxide scale and protect the uranium silicide matrix. As a result of powder metallurgy approaches, the SPS densified pellets show improved microstructure and homogeneous distribution of the Cr additives through the U₃Si₂ fuel matrix than the arc-melted alloys. The SPS densified Cr-doped pellets also show much-improved oxidation and corrosion resistance in both dynamic oxidation and steam corrosion environments under relevant reactor operating conditions. These results highlight the significance in the microstructure control and elemental homogeneity of additives through the fuel pellets in order to improve materials' corrosion resistance.

2. Experimental details

2.1. Powder preparation and spark plasma sintering

The as-received U₃Si₂ powders were prepared at INL. Near

stoichiometric quantities of uranium and silicide elements were pressed and then agglomerated, followed by arc melting [3]. Chromium powders were purchased from Sigma-Aldrich Inc (St. Louis, Missouri, USA), with a mesh of ~325 µm. HEBM was used to reduce the grain size, improve the sinterability, and allow uniform mixing of the starting powders. The HEBM apparatus used in the current work is a planetary micro mill (Pulverisette 7, Idar-Oberstein, Germany). Both the milling jar and the milling ball were made of tungsten carbide (WC), and the diameter of the ball is ~8 mm. A typical ball milling cycle included 15-minutes milling time and 10-minutes idling time, and the rotating speed was set to 500 rounds per minute. U₃Si₂ and Cr powders were ball milled separately for various cycles and then mixed for 4 cycles before consolidation.

An SPS apparatus (Fuji, Dr. Sinter SPS 211-LX, Saitama, Japan) was used to perform the sintering, the procedure of which included two heating stages with heating rates being 150 °C/min and 100 °C/min, a holding stage of 5 min., and a free cooling stage. Prior to the sintering, a piece of graphite foil was used to wrap the inner side of a graphite die, then 1 g of homogeneously mixed U₃Si₂ + Cr powders were loaded to the die, two ends of which were then plugged by two graphite punches. The assembly was subsequently wrapped with a piece of felt to reduce heat loss, placed in the middle of the sintering chamber. A thermocouple was placed in a hole on the wall of the die to measure the temperature and control the sintering process. A pressure of 40 MPa was loaded on the assembly during the sintering period, and after consolidation, the load was instantly released to avoid pellet cracking. The as-sintered pellets were ground and polished with silicon carbide papers and diamond paste. Archimedes' method was used to measure specimens' physical density, and theoretical density was calculated based on the mass fraction of the dopant and the matrix.

2.2. Microstructure and mechanical properties characterization of Cr-doped U₃Si₂

The microstructure of the as-sintered Cr-doped U₃Si₂ pellets was characterized by a field-emission scanning electron microscopy (SEM, Carl Zeiss Supra 55, Jena, Germany) and an FEI Versa 3D (Oregon, US). Chemical characterization of the as-sintered pellets and the surface after steam corrosion was conducted with the SEM integrated with an energy-dispersive X-ray spectroscope (EDS, Oxford, UK). After the steam test, the phases of the corroded surface were determined by X-ray diffraction (XRD) using a Panalytical X'Pert XRD system (Westborough, Massachusetts) with Cu K α irradiation. The wavelength is 1.5406 Å. The scanning step was set to 0.05° with a scanning rate of 2 s/step and a scanning range of 20° to 80°. The mechanical properties of the SPS densified Cr-doped pellets were characterized using a Leco M-400 Microhardness tester. The hardness and fracture toughness were determined following the procedure reported in a previous study [9].

2.3. Dynamic oxidation testing and steam corrosion

Dynamic oxidation of the SPS-densified Cr-doped pellets was evaluated using a thermogravimetric analysis (TGA) apparatus, which continuously measured the heat flow and sample weight during the testing period. The apparatus uses a simultaneous differential scanning calorimetry (DSC) / TGA system (SDT650, thermal analysis (TA) instrument, Delaware). For each test, a piece of sample weighing 20–30 mg was loaded to an alumina crucible, which was then put in the chamber of the apparatus. An empty crucible was also loaded as the reference. For a typical ramping test, the specimen was heated with a heating rate of 10 °C/min up to 1000 °C. Isothermal annealing was also performed on the sintered pellets at 300 °C for 2 hours before further heat up. The normalized heat flow and weight change plotted vs. time or temperature allowed the determination of the onset temperature and oxidation kinetics. The steam oxidation testing was performed by a NETZSCH F3 simultaneous thermal analyzer (STA). The sample

chamber was connected to a water vapor generator. The water vapor was injected at a rate of 5 g/hour. The sample was placed on a plate-type sample holder such that it was fully exposed to the water vapor. The temperature was calibrated by the indium, bismuth, aluminum, and gold standards.

3. Results and discussions

3.1. Microstructure, phase, and mechanical properties of the Cr-doped U_3Si_2

Dense U_3Si_2 pellets of various compositions with 3, 5, and 10 wt% Cr additives were prepared by HBEM and SPS. Table 1 summarizes all samples prepared by SPS, along with their sintering conditions and measured physical densities. Different ball milling cycles starting from as-received Cr powders, 20 and 40 cycles were applied to control the powder size of Cr and its distribution through the silicide matrix. U_3Si_2 powder ball-milled for 20 cycles in sample 1 were also applied to achieve a nano-sized U_3Si_2 matrix in the final sintered body. Micron-sized U_3Si_2 (referred to as mc- U_3Si_2 hereinafter) pellets were achieved by using 4-cycle milled U_3Si_2 . The powder mixture of the Cr and U_3Si_2 was further milled for an additional 4 cycles in order to mix them uniformly before SPS consolidation. All of the SPS-densified pellets achieve a physical density above 95 TD%. The 3 wt% and 5 wt% Cr-doped U_3Si_2 specimens have an 11.3 % and 8.2 % increase in uranium densities, while the 10 wt% Cr-doped U_3Si_2 has similar uranium density as comparing to UO_2 . This suggests that Cr-doped U_3Si_2 maintains an enhanced uranium density over UO_2 , which is beneficial to improve fissionable content [19], increase burnup [20] and elongate the cycle length [3].

Fig. 1(A) and (B) show the SEM images of the 5 wt% (sample 2) and 10 wt% (sample 3) Cr-doped mc- U_3Si_2 pellets after SPS consolidation, respectively. No pre-processing of the Cr powders is conducted, and thus the particle size of the Cr additives is within several tens of microns, as shown in the SEM images. Despite the relatively large particle size, the Cr additives were embedded reasonably uniformly in the dense U_3Si_2 matrix, and no significant pores can be identified in the sintered pellet. In contrast, the U_3Si_2 (Al, Cr, Y) alloys prepared by arc melting showed poor uniformity with distinct and separate two phase assemblies, and the separate assemblage of metal additives may not be very beneficial to protect the U_3Si_2 grains. In addition, phase segregation and impurities were also observed in the pellets prepared by arc melting. For the Mo-doped U_3Si_2 pellets sintered by Lopes [6], although SPS was used to synthesize specimens, nano-size pores and phase impurities can still be observed in the pellets with an inhomogeneous microstructure of numerous inclusions near grain boundaries. Johnson et al. [21] reported the synthesis of UN- U_3Si_2 composite fuels, where a highly heterogeneous structure was observed with multiple inclusions of U_3Si_2 , U_3Si_5 , and UN in different regions. A homogeneous distribution of metal additives, ideally at the grain boundaries of U_3Si_2 , will be useful in order to enhance oxidation/corrosion properties and pellet integrity. Powder

Table 1
Summary of sample details for Cr-doped U_3Si_2 .

Sample	Sample compositions (weight %)	Sintering conditions (°C, mins)	Density (g/cc), TD%
1	97 % 20-cycle U_3Si_2 , 3 wt% 40-cycle Cr	1,000, 10 min	11.37, 95.2 %
2	95 % mc- U_3Si_2 , 5 wt% as-received Cr	1,000, 5 min.	11.28, 95.7 %
3	90 % mc- U_3Si_2 , 10 wt% as-received Cr	1,000, 5 min.	10.85, 95.2 %
4	90 % mc- U_3Si_2 , 10 wt% 20-cycle Cr	1,000, 5 min.	10.98, 96.3 %
5	90 % mc- U_3Si_2 , 10 wt% 40-cycle Cr	1,000, 5 min.	11.02, 96.8 %

metallurgy approaches, e.g., by SPS in the current study, clearly show distinct advantages as compared with arc-melting.

A close-up SEM image is shown in Fig. 1B, displaying a distinct phase with grey contrast between Cr additives and matrix, suggesting a possible interaction between Cr and U_3Si_2 . Fig. 1C shows the XRD patterns of the 5 wt% and 10 wt% Cr-doped samples. In addition to the U_3Si_2 (indexed by a JCPDS No. 07-015-1962) and Cr, a ternary phase of $UCr_{1.375}Si_{0.625}$ can be identified and indexed by a JCPDS No. 04-008-4392 (not shown here). In a relevant study on oxidation of U_3Si_2 -Cr alloys prepared by arc melting [18], $UCr_{1.375}Si_{0.625}$ was also identified from the as-prepared specimen.

EDS elemental analysis, as shown in Fig. 2A, was performed by spot measurements on the phases showing distinct contrasts. The phase with the darkest contrast consists of Cr. The matrix (spot 2) consists of U, Si, and O, with the atomic ratio between U and Si is 3:2, suggesting that the dominant phase in the sintered pellet is U_3Si_2 . The constituent elements of the intermediate phase between Cr additives and U_3Si_2 matrix are U, Cr and Si. Quantitative analysis suggests that the composition of the ternary phase is close to $UCr_{1.375}Si_{0.625}$, consistent with the XRD results. In all of the EDS analysis, oxygen elements were also identified. It is noted that the powder process and SPS consolidation were performed in an environmentally controlled glovebox with oxygen and moisture levels below 1 ppm. Therefore, the oxygen elements identified by EDS may be attributed to the surface oxidation after taking the sintered pellets out of the glovebox and during sample preparation for SEM and EDS characterization. These are consistent with the expectation that both U_3Si_2 and Cr can easily form oxide scales in ambient conditions.

Fig. 3 shows SEM images of the micro-indentations generated on the surfaces of three Cr-doped U_3Si_2 pellets (samples 1–3), and the mechanical testing results are summarized in Table 2, along with the mechanical properties of monolithic mc- U_3Si_2 [9] for comparison. The micro-hardness and the fracture toughness of each sample are plotted in Fig. 3D for better visualization. In general, the hardness of the Cr-doped U_3Si_2 is within the range of 6.5–7.5 GPa, slightly higher than that of the monolithic U_3Si_2 (~6.1 GPa). The addition of Cr additives increases the hardness of the composite pellets, consistent with a previous observation of Cr doping in Fe₂B [22]. Fracture toughness of the specimens generally lies within the range of 2–3.4 MPa m^{1/2}. When doping with 3 wt% and 5 wt% Cr, the fracture toughness of the composite pellets decreases slightly as compared with that of monolithic U_3Si_2 (~3.2 MPa m^{1/2}). Further increasing the Cr additive to 10 wt%, the fracture toughness increases to ~3.4 MPa m^{1/2}. Crack propagation can be observed in the lower Cr-doped samples, but cracks are barely observed in the 10 wt% Cr-doped pellet, suggesting that the 10 wt% Cr-doped U_3Si_2 are both mechanically strong and tough. Conclusive results cannot be drawn on the impacts of the Cr-doping on mechanical properties based on nano-indentation testing results. The effect of the ternary phase formation, particularly in the higher Cr-doped pellets, on the mechanical properties is not clear. Nevertheless, all of the Cr-doped U_3Si_2 pellets had significantly higher fracture toughness than oxide fuel pellets. In particular, the 10 wt% Cr-doped fuel has the highest fracture toughness, beneficial to mitigate fuel cladding mechanical interaction during reactor operation. The high mechanical properties, particularly fracture toughness, will be useful to increase the oxidation and corrosion resistance due to the improved resistance against crack propagation, which is demonstrated by the results of steam testing for 10 wt% Cr-doped U_3Si_2 pellets.

3.2. Dynamic oxidation behavior of the Cr-doped U_3Si_2

The dynamic oxidation behavior of the SPS densified Cr-doped U_3Si_2 fuel pellets was tested using a TGA, as shown in Fig. 4, and the onset oxidation temperature and weight gain for each sample are summarized in Table 3. The onset oxidation temperature of the Cr-doped pellets with different Cr amounts from 3 wt%, 5 wt%, and 10 wt% are generally similar within the range of 530–550 °C, significantly higher than the

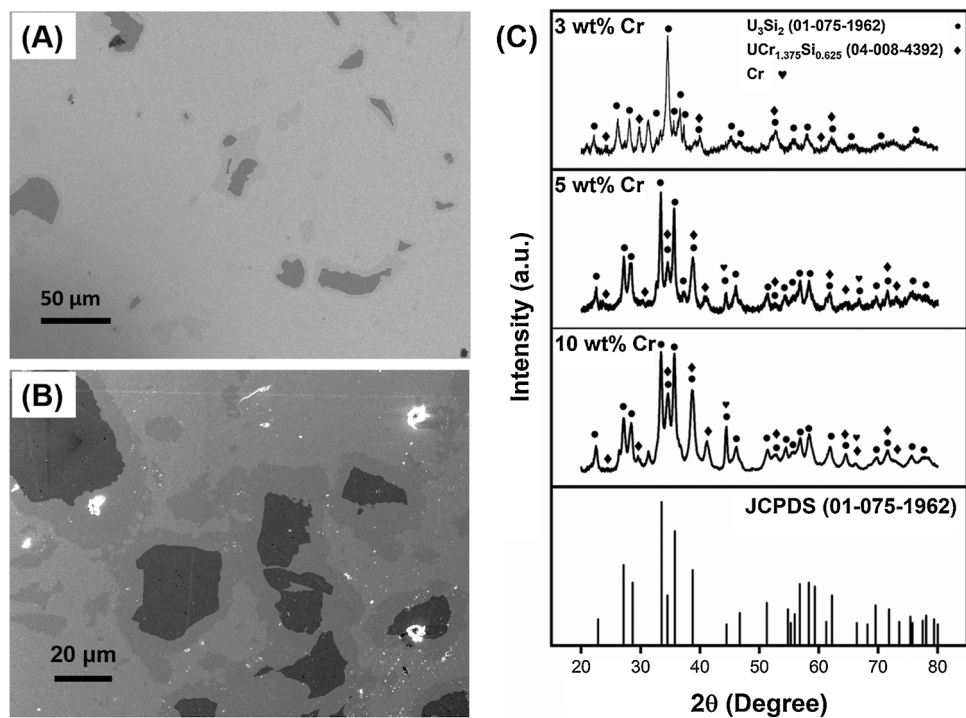


Fig. 1. SEM images of (A) 5 wt% Cr-doped, and (B) 10 wt% Cr-doped U₃Si₂ pellets sintered by SPS. No obvious pores were found, and large-sized Cr particles were homogeneously distributed inside the U₃Si₂ matrix. (C) XRD patterns of the SPS-sintered Cr-doped U₃Si₂ pellets, along with the JCPDS card for U₃Si₂. Three major phases can be identified, i.e., U₃Si₂, Cr, and UCr_{1.375}Si_{0.625}.

results reported previously for the pellets prepared by arc melting [18]. The onset temperature increases slightly with the increase of Cr doping amount, indicating a positive effect of Cr doping to improve the oxidation resistance of U₃Si₂. The oxidation rates are generally similar for the Cr-doped samples, slightly increasing with the amount of Cr doping as evidenced by the steep slope in the oxidation curve accompanying with a sharply rising heat flow profile for the 10 wt% Cr-doped sample. The terminal oxidation weight gains for all of the samples tested are generally within 19–22 wt%, as tabulated in Table 3.

To fully utilize the Cr additive to further improve the oxidation resistance of the Cr-doped pellets, isothermal annealing in air was performed at 300 °C for 2 hours, below the onset oxidation temperature for U₃Si₂, and thus no significant oxidation was expected for silicide fuel matrix. By deliberately oxidizing Cr additives to form oxide scale serving as a protective measure, the oxidation resistance of the annealed pellets can be further improved. The dynamic ramping test shown in Fig. 4B indicates that after thermal annealing, all three samples (3 wt%, 5 wt%, and 10 wt%) have an increased onset temperature for oxidation up to 550 ~ 570 °C. These results clearly indicate the beneficial effects of inducing oxide scales to improve oxidation resistance despite no significant variation in the oxidation rate and terminal oxidation weight gain. It is of significance to achieve similar oxidation resistance with minimized Cr doping, which will be beneficial to maintain a high fissile element density of the silicide fuel when used as AFT for LWRs.

We also explored the possibility of further improving the oxidation resistance of the SPS densified Cr-doped U₃Si₂ by reducing the particle size of Cr additives and optimizing their distributions in the fuel matrix. Two additional specimens (samples 4 and 5) were prepared, with various ball milling cycles for Cr (20 and 40 cycles) before mixture with U₃Si₂. As shown in Fig. 4C, with the same Cr doping amount but different ball milling cycles (thus expected finer particle sizes), the onset temperature is further improved to 570 °C from 533 °C for the 10 wt% Cr-doped pellet without annealing in which the Cr additive was ball milled for 20 cycles. A similar observation can be found for the pellets with 10 wt% Cr additives pre-milled for 40 cycles. Therefore, additional

ball milling to reduce particle sizes of Cr can further increase the onset oxidation temperature. The positive impact of reducing particle size could result from the better distribution of the smaller-sized Cr in the U₃Si₂ matrix, promoting the formation of ternary phase. Additionally, Cr additives with reduced particle size with a better distribution in the grain boundary of U₃Si₂ could enable the easy formation of the oxide scale, leading to a better oxidation resistance property. Isothermal annealing after sintering to create an oxide scale is an effective strategy to further improve the oxidation performance of the Cr-doped composite pellets. On the other hand, the additional ball milling will add a small energy penalty for processing the powders.

3.3. Steam corrosion of the Cr-doped U₃Si₂

3.3.1. Ramping testing in steam

Dynamic oxidation behavior of the 5 wt% and 10 wt% Cr-doped U₃Si₂ pellets (samples 2 and 3) was examined with ramping testing under high-temperature steam, along with the monolithic U₃Si₂ [3] prepared by vacuum sintering at Idaho National Laboratory (INL) for comparison. All samples were tested by a simultaneous thermal analyzer at Westinghouse, and the weight gain resulting from steam oxidation was recorded. For the monolithic U₃Si₂ pellet prepared by vacuum sintering at INL [3], a sudden weight loss occurred when the steam temperature reached 450 °C, due to the fragmented pieces expelled out of the plate-type crucibles during steam testing. This is similar to previous observations [23] on monolithic U₃Si₂ tested under steam, in which the sample experienced rapid mass loss starting from ~460–480 °C. For the U₃Si₂-Cr prepared by arc melting [18], Wood et al. stated that the onset temperature of the fuel was in the range of 426 to 451 °C, and the onset temperature firstly increased with the amount of Cr and then decreased afterward.

For the 5 wt% Cr-doped U₃Si₂ pellet, fragmentation during steam oxidation testing also occurred. The fragmentation pieces were collected after testing, as shown in Fig. 5A. An oxidation layer is noticeable on the surface of the pellet, showing darker contrast. The thermo-gravimetric

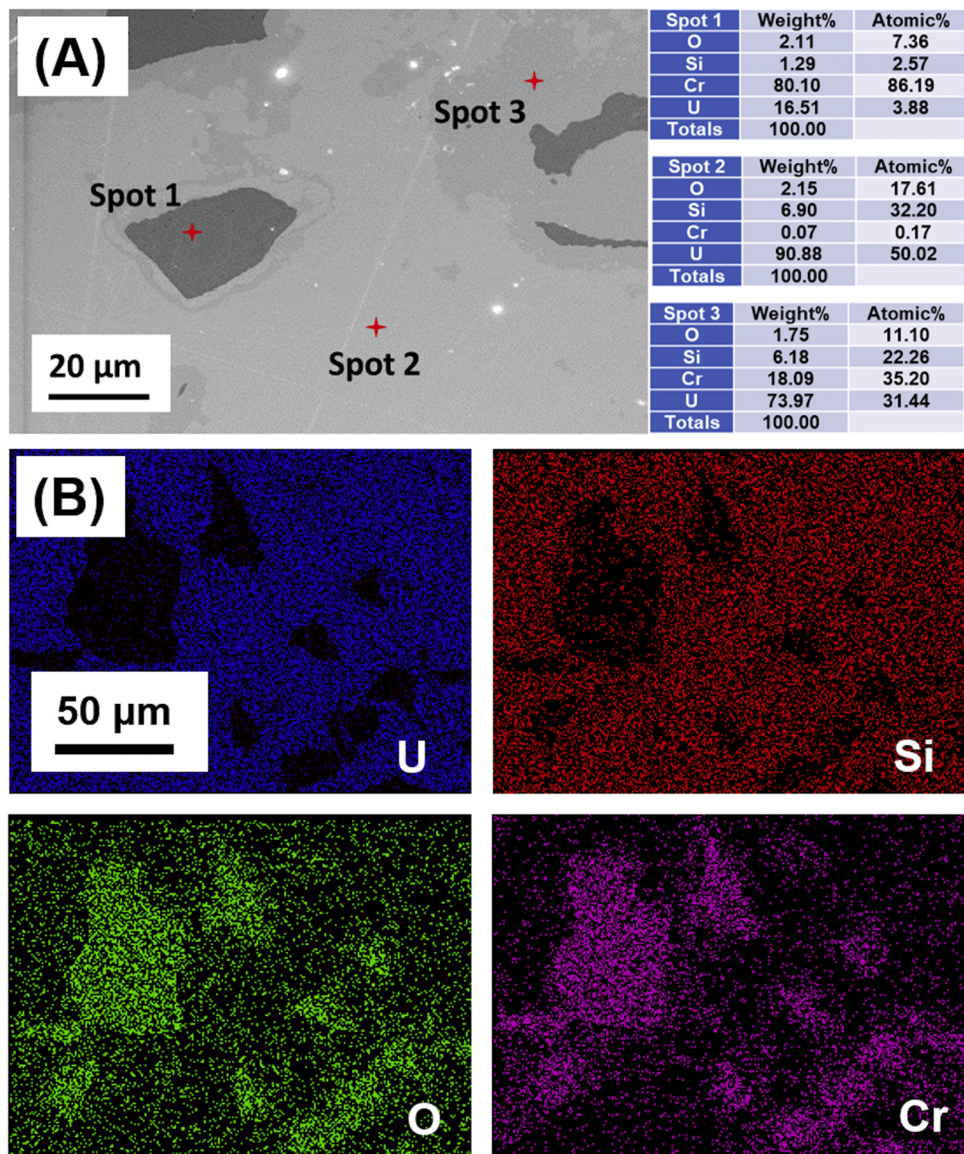


Fig. 2. (A) EDS point scan results showing three phases with distinct contrasts, with spot 1 being oxidized Cr, spot 2 being oxidized U_3Si_2 , and spot 3 being oxidation product of a ternary phase composed of U, Si, and Cr. (B) EDS mapping confirms that the matrix consists of U and Si, and the additive is oxidized Cr.

analysis shown in Fig. 5B indicates that no oxidation occurs at the temperature of 520 °C, which is about 70~100 °C greater than that observed for monolithic U_3Si_2 prepared by vacuum sintering and the Cr-doped U_3Si_2 prepared by arc melting. This is consistent with better oxidation resistance of the SPS densified Cr-doped U_3Si_2 under dynamic ramp testing in air, as evidenced by the higher onset oxidation temperature (see Table 3).

For the as-sintered 10 wt% Cr-doped U_3Si_2 pellet, weight gain occurred at the temperature of 520 °C in the steam ramping test condition, further confirming improved oxidation resistance in steam for the SPS-densified pellets as compared with previous studies [18]. The improved oxidation resistance could be attributed to the better distributed Cr metal additives in the U_3Si_2 matrix and better fracture toughness against crack propagation for this particular sample than Cr-doped pellets prepared by arc melting [18]. After reaching the onset temperature, a continuous weight gain of up to 17 wt% was observed, and the oxidation process lasted until 850 °C. It is expected that the oxidation continues to reach full oxidation at higher steam testing temperature. This result also indicates a much slower oxidation rate when testing in the steam oxidation environment as compared with the dynamic

oxidation testing in air in which full oxidation is reached about 600 °C. Note sudden weight loss was observed due to expelled fragmented pieces during the test of the INL sample [3]. The improved corrosion resistance by ramp testing in steam for the 10 wt% Cr-doped U_3Si_2 pellet may be associated with better fracture toughness of materials to mitigate large thermal stress generated during the extensive exothermic reaction.

3.3.2. Isothermal oxidation testing in steam

Different from the ramping test in steam, the isothermal oxidation was performed under steam at a constant temperature of 360 °C, the rim temperature of the fuel pellet experienced during the reactor operation. The isothermal oxidation testing in steam was performed on the 10 wt% Cr-doped pellets and the INL sample prepared by vacuum sintering for comparison. After 24-hour isothermal steam testing, the Cr-doped sample still maintained its integrity with barely any change in its mass. In contrast, the monolithic pellet prepared by vacuum sintering at INL experienced rapid weight loss after 6 hours, suggesting significant oxidation and loss of the fragmented pieces out of the crucible. For the 10 wt% Cr-doped pellet after exposed to steam for 24 hours, no obvious fracture was observed, and the sample still possessed its original luster.

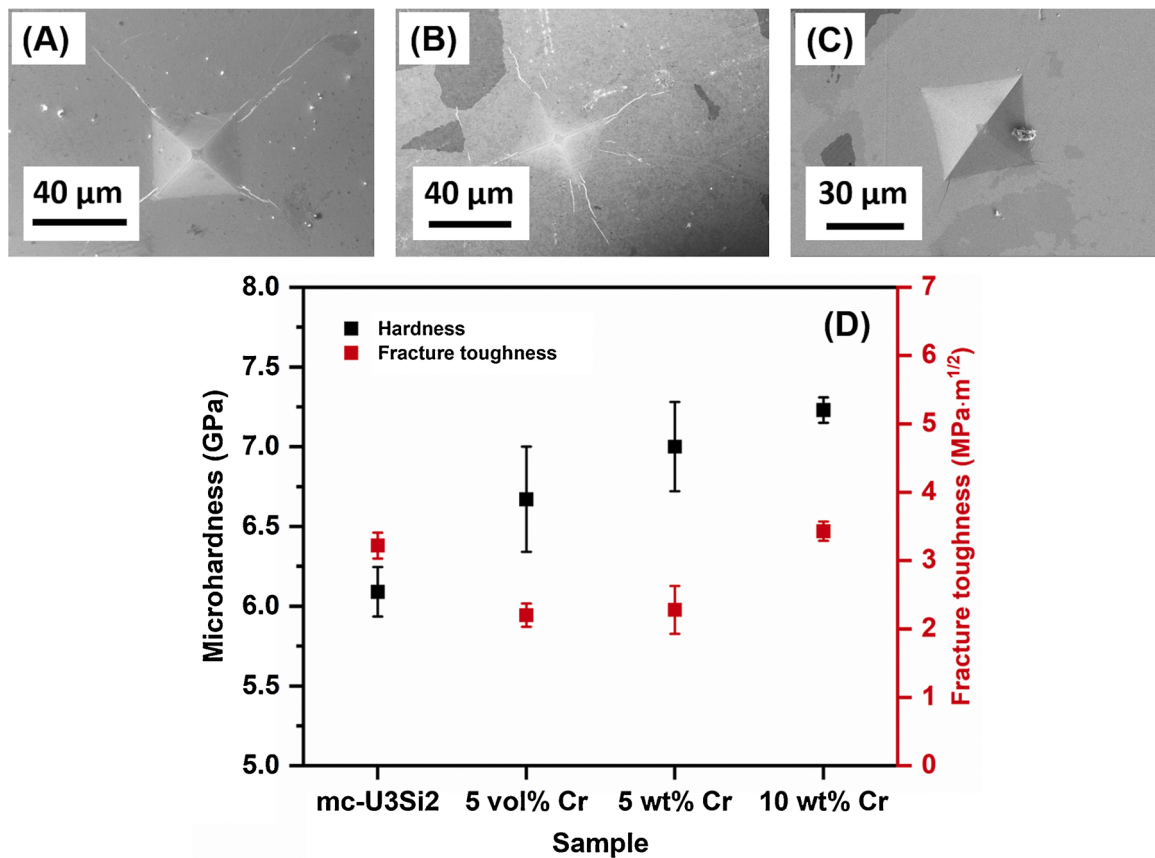


Fig. 3. SEM images showing microindentation on the surface of (A) 3 wt% Cr-doped U₃Si₂, (B) 5 wt% Cr-doped U₃Si₂, and (C) 10 wt% Cr-doped U₃Si₂. (D) measurements of microhardness and fracture toughness of U₃Si₂ specimens with various additions of Cr, along with microcrystalline U₃Si₂ for comparison.

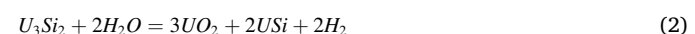
Table 2
Summary of mechanical properties of Cr-doped U₃Si₂ Sintered at 1000 °C.

Sample (No.)	Sample compositions (weight %)	Hardness (GPa)	Fracture toughness (MPa·m ^{1/2})
mc-U ₃ Si ₂ [9]	Monolithic mc-U ₃ Si ₂	6.1 ± 0.2	3.5 ± 0.2
1	97% 20-cycle U ₃ Si ₂ , 3 wt% 40-cycle Cr	6.7 ± 0.3	2.2 ± 0.2
2	95 % mc-U ₃ Si ₂ , 5 wt% as-received Cr	7.0 ± 0.3	2.3 ± 0.4
3	90% mc-U ₃ Si ₂ , 10 wt% as-received Cr	7.2 ± 0.1	3.4 ± 0.1

Partial oxidation patches with a dark contrast were found on the surface of the pellet. A previous study [15] also reported that U₃Si₂ was completely pulverized when tested in an isothermal steam condition at 400 °C for 4 hours. Wood et al. [18] performed a similar isothermal steam testing for U₃Si₂+Cr alloys manufactured by arc melting. A significant weight gain of over 12 wt% was reported for 7 vol% Cr-doped U₃Si₂ by arc melting after less than 6 hours at 350 °C before weight loss occurred, due to the material ejected out of the crucible. U₃Si₂ pellets doped with 5.5 vol% Cr and 2.2 vol% Cr experienced rapid weight gain after exposure to steam corrosion at 350 °C for 4 hours. These comparisons clearly demonstrate a significantly improved steam corrosion resistance for the 10 wt% Cr-doped pellet manufactured by SPS. It is of significance as the first promising result to demonstrate the excellent structural integrity of the U₃Si₂ pellets under the steam testing condition and a relevant reactor operation temperature.

3.3.3. Microstructure and phase evolution of the Cr-doped pellets under steam corrosion

The microstructure and phase variation of the Cr-doped U₃Si₂ pellets after steam corrosion testing were characterized by SEM, EDS and XRD for both 5 wt% Cr-doped pellet ramped up to 520 °C and the 10 wt% Cr-doped pellet held at 350 °C for 24 hours, in order to understand the oxidation process under steam corrosion. For the 5 wt% Cr-doped pellet with the steam ramping test to 520 °C, full oxidation did not occur. However, the characterization of this specimen still provides useful information in understanding phase changes and possible oxidation products at the early stage of oxidation. For both pellets, the oxidation products can be generally indexed as UO₂, U₃O₈, SiO₂, USi₃, Cr₂O₃, and UCr_{1.375}Si_{0.625}, which can be confirmed from XRD patterns in Fig. 6. The oxidation of U₃Si₂ under steam is a very complex process, which involves multiple reactions such as the oxidation of U, Si, and Cr and the reaction between U₃Si₂ and H₂ [23]. Wood et al. [18] conducted chemical equilibrium calculations and stated that the primary and secondary reactions of U₃Si₂ with steam were expected to be either reaction 1 and 2, or reactions 1 and 3. The authors also stated that U₃O₈ would not form in large amount due to lack of oxidants, which is in accordance with our analysis of the oxidation products formed under steam testing.



The microstructure of the oxidation layer for the 5 wt% Cr-doped pellets can be observed from the SEM images at different magnifications as shown in Fig. 7A. The oxidation layer shows bright contrast and covers only part of the pellet surface, indicating limited oxidation on the

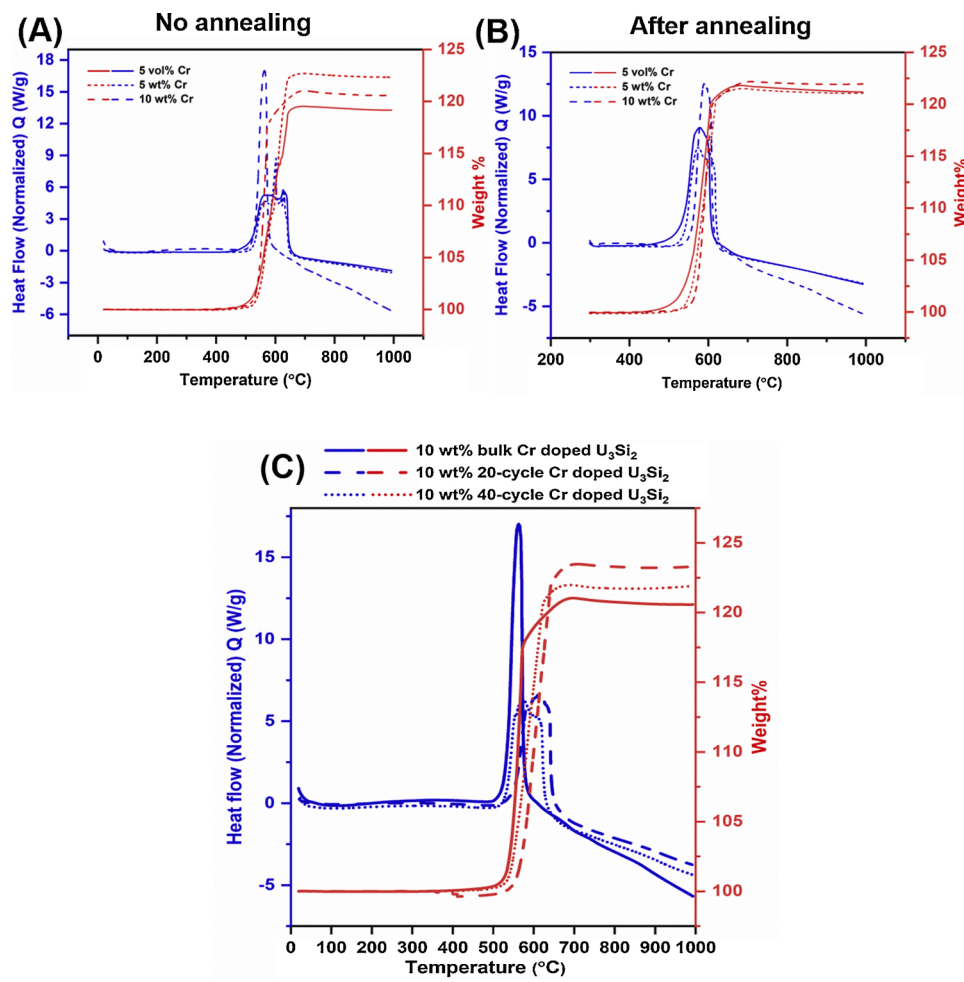


Fig. 4. Dynamic thermos-gravimetric ramping tests in air showing oxidation behavior of Cr-doped U_3Si_2 samples with various Cr additions (A-B) and particle sizes (C). Without annealing, 3 wt% and 5 wt% Cr-doped U_3Si_2 show similar behaviors, which are better than the sample with 10 wt% Cr-doped pellet. After annealing at 300 °C for 2 hours, all samples show improved onset temperature as a result of the formation of Cr oxide scales in the U_3Si_2 matrix. For samples with the same amount of Cr addition, reducing particle size of Cr can improve the oxidation resistance of the sample slightly.

Table 3
Summary of Oxidation Behavior of Cr-doped U_3Si_2 Samples Sintered at 1000 °C.

Specimens	Annealing	Onset temperature (°C)	Time to full oxidation (min)	Terminal Oxidation (%)
20-cycle U_3Si_2 , 3 wt% 40-cycle Cr	No	520	13	19.0
20-cycle U_3Si_2 , 3 wt% 40-cycle Cr	Yes	550	13	21.3
mc- U_3Si_2 , 5 wt% as-received Cr	No	540	21	22.5
mc- U_3Si_2 , 5 wt% as-received Cr	Yes	555	19	21.1
mc- U_3Si_2 , 10 wt% as-received Cr	No	530	23	21.0
mc- U_3Si_2 , 10 wt% as-received Cr	Yes	570	18	22.0
mc- U_3Si_2 , 10 wt% 20-cycle Cr	No	570	18	23.2
mc- U_3Si_2 , 10 wt% 40-cycle Cr	No	545	18	22.0

sample surface. The surface scratches are still observable for the un-oxidized area (see a large view from the inset of Fig. 7A), suggesting a well-maintained pellet integrity. To further characterize the oxidation products and microchemistry variation of the pellet after steam corrosion ramped to 520 °C, EDS elemental mapping was performed, as shown in Fig. 7B. From the EDS mapping, it is noticed that the element U can be detected on the whole scanning area, complementary to the Cr mapping, suggesting the dominant U_3Si_2 phases and Cr-enriched phases. Cr additives are found to uniformly distribute through the matrix, which has been oxidized during the tests. Si, on the other hand, is enriched in the central regime of the map, corresponding to the un-oxidized surface with the dark contrast shown in Fig. 7A. A small amount of Si can be detected in the region away from the central area, which suggests that the oxidation layer contains a low ratio of Si. Oxygen can be detected almost everywhere, except for the central part of the scanning area, consistent with Si elemental mapping. Comparing to the arc-melted U-Si-Cr alloys that experience mass loss around 450 °C [18], the SPS-sintered pellets display superior stability and exceptional oxidation resistance.

Fig. 7C and D show the SEM image and EDS elemental mapping of the preserved 10 wt% Cr-doped pellet, which displays excellent pellet integrity, after steam corrosion testing at 350 °C for 24 hours. Only minimum oxidation can be observed in the limited surface patch areas, and the majority of the pellets are intact, showing original surface features with polished scratches clearly identified. The corresponding EDS elemental mapping suggests that the matrix of the tested specimen consists of U, Si, and O elements, which are the oxidation products of U_3Si_2 and Cr. Cr additives are evident from the mapping, similar to the

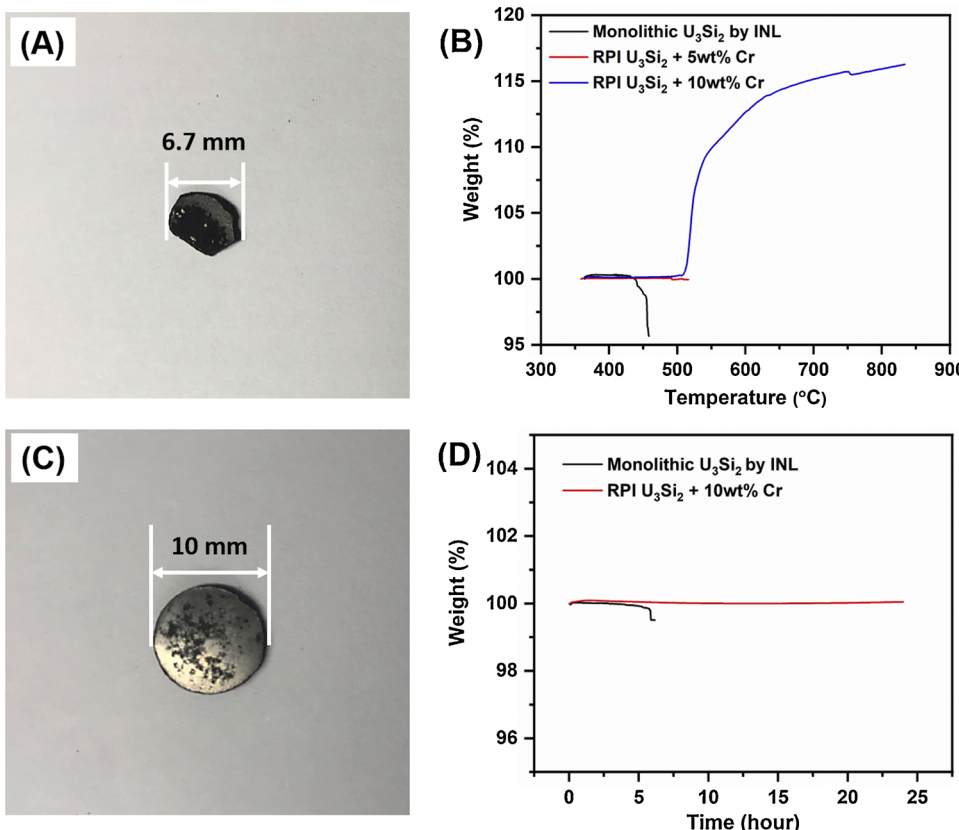


Fig. 5. (A) A preserved specimen of the 5 wt% Cr-doped U_3Si_2 after steam ramping test; (B) Dynamic thermogravimetric ramping test in steam until mass loss, shows the onset temperature of 5 wt% and 10 wt% Cr-doped U_3Si_2 is around 520 °C. The monolithic sample prepared by vacuum sintering at INL experienced rapid mass loss at ~ 440 °C. The 10 wt% Cr-doped U_3Si_2 pellet reacts with H_2O until up to 850 °C; (C) A preserved specimen of the 10 wt% SPS-densified Cr-doped U_3Si_2 pellet showing exceptional pellet integrity and preserving the original luster without noticeable weight gain after steam oxidation testing at 360 °C for 24 hours ; and (D) Dynamic thermogravimetric isothermal test in 360 °C steam. The monolithic sample prepared by vacuum sintering at INL experiences rapid mass loss at ~ 5 hours.

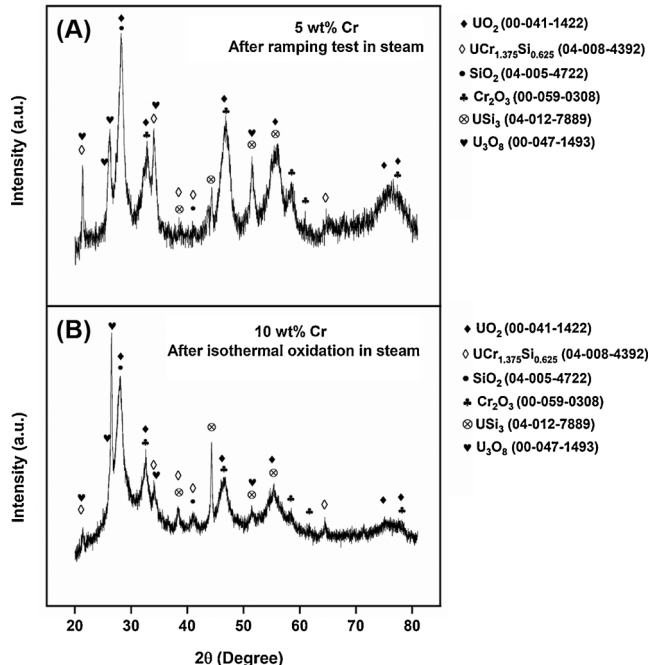


Fig. 6. XRD patterns of the preserved Cr-doped U_3Si_2 samples after dynamic thermogravimetric test in steam, with (A) 5 wt% Cr-doped sample after ramping test and (B) 10 wt% Cr-doped sample after isothermal oxidation test. Multiple phases can be identified including UO_2 , $\text{UCr}_{1.375}\text{Si}_{0.625}$, SiO_2 , Cr_2O_3 , USi_3 , and U_3O_8 .

sample with 5 wt% Cr. In addition to the oxide patches from the selected area, oxygen elements can also be observed from the area without the oxide scale, resulting from the surface oxidation of the uranium silicide. Comparing to the arc-melted U-Si-Cr alloys that pulverized after 3.3 hours (5.5 vol% Cr) or 6.6 hours (7 vol% Cr), the SPS-sintered pellets exhibit great oxidation resistance that can last for at least 24 hours with minimum surface oxidation. This demonstrates the significance of microstructure control when preparing doped U_3Si_2 fuels. Comparing the results from the dynamic ramping and the isothermal steam testing, larger area of oxidation scale can be found in the 5 wt% Cr-doped sample ramped tested at 520 °C. The oxidation scale of isothermal testing is scattered and sparse for the 10 wt% Cr- U_3Si_2 at a lower temperature (350 °C) but significantly longer duration (24 hours). This result can be attributed to different oxidizing approaches, since in the ramping test the specimen experiences much higher temperature.

4. Conclusions

In summary, Cr-doped U_3Si_2 fuel pellets with various Cr contents and Cr particle sizes were sintered with SPS at 1000 °C for 5 mins. Dense and uniform pellets were obtained, and their microstructures and phase compositions were extensively characterized with SEM, XRD, and EDS. Mechanical properties and oxidation resistance of all specimens were measured with micro-indentation testing and TGA analysis, respectively, and were compared with the undoped pellets. The onset temperatures of the SPS densified Cr-doped pellets are generally within 530–550 °C, which can be further improved to 570 °C by isothermal annealing in the air to create a protective Cr_2O_3 oxide scale. Ball milling of the starting metal additives can help to further increase the onset temperature for oxidations, probably due to a better distribution of finer Cr additives throughout the U_3Si_2 matrix. Steam ramp testing and isothermal thermal annealing at relevant steam corrosion conditions show the much-improved oxidation and corrosion resistance of the SPS

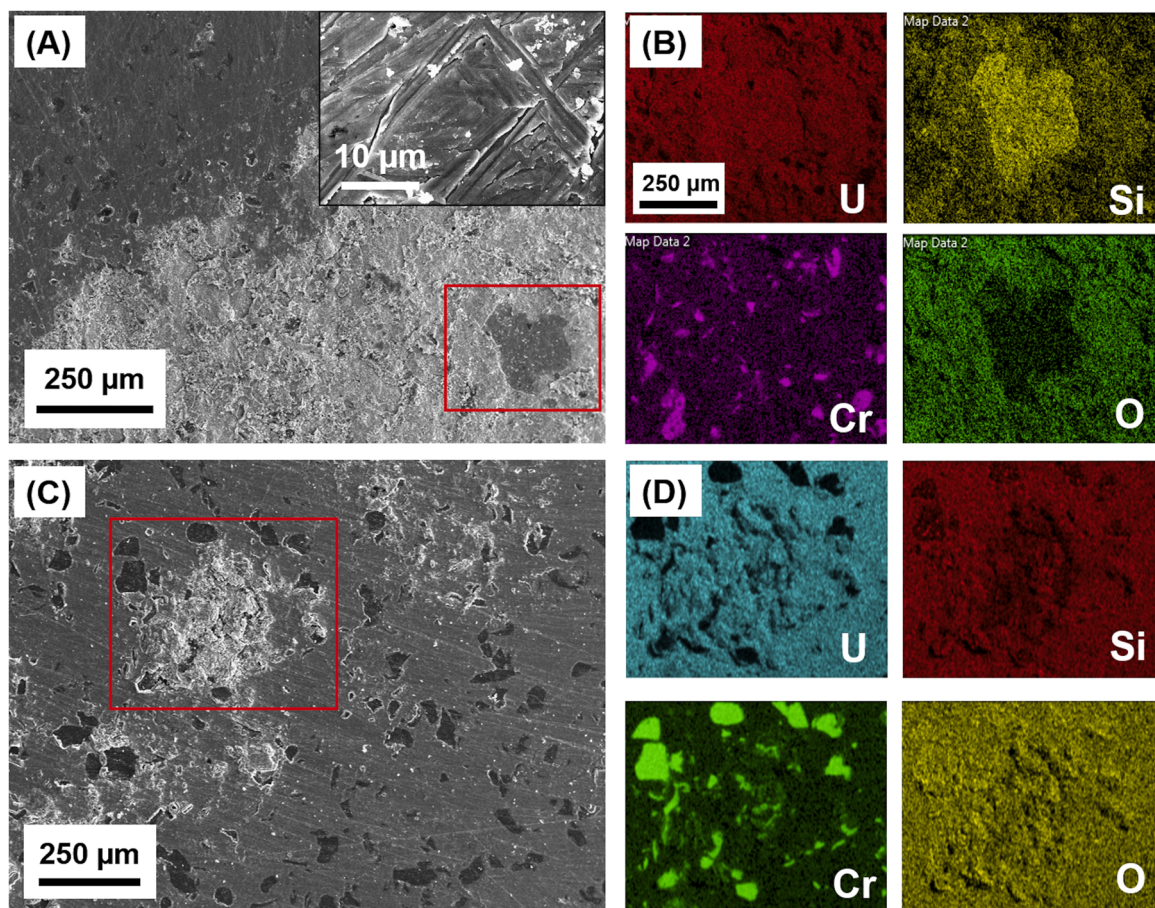


Fig. 7. (A) SEM images showing limited oxidation on the preserved 5 wt% Cr-doped U_3Si_2 specimen after dynamic ramping test in steam up to 520 °C. Original surface scratches can be clearly observed, suggesting a well-maintained pellet integrity. (B) EDS elemental mapping of the selected area showing limited oxidation on the surface of the fuel pellet. The oxidation scale is uranium enriched and silicon depleted. (C) A SEM image showing scattered oxidation scales on the preserved 10 wt% Cr-doped U_3Si_2 specimen after an isothermal steam test at 350 °C for 24 hours. The oxidation region is sparse and discontinuous, suggesting less oxidation comparing to the previous sample. (D) EDS mapping of the selected area showing the distribution of the Cr-additives. In addition to the oxide patches from the selected area, oxygen elements can also be observed from the area without oxide scale, resulting from the surface oxidation of the uranium silicide pellets taken out from the environmentally-controlled glovebox.

densified pellets as compared with the U_3Si_2 and Cr-doped pellets fabricated by vacuum sintering or arc melting. The onset oxidation temperature in ramping testing in steam is above ~520 °C for Cr-doped U_3Si_2 with a reduced oxidation rate to achieve full oxidation. Isothermal steam tests further confirm the excellent oxidation resistance of the 10 wt% Cr doped U_3Si_2 specimen, which maintains an excellent material integrity for at least 24 hours at 360 °C. These results demonstrate the possibility of using alloying additives as an effective strategy to improve the corrosion resistance and structural integrity of the U_3Si_2 to enable their potential application as promising ATFs for reactor operation.

Data availability

Data will be made available on request.

CRediT authorship contribution statement

Bowen Gong: Conceptualization, Investigation, Visualization, Writing - original draft, Writing - review & editing. **Lu Cai:** Investigation, Visualization, Writing - review & editing. **Penghui Lei:** Investigation, Visualization, Writing - review & editing. **Kathryn E. Metzger:** Resources, Investigation, Writing - review & editing. **Edward J. Lahoda:** Resources, Investigation, Writing - review & editing. **Frank A. Boylan:** Resources, Writing - review & editing. **Kun Yang:** Investigation, Writing - review & editing. **Jake Fay:** Investigation, Writing -

review & editing. **Jason Harp:** Writing - review & editing. **Jie Lian:** Conceptualization, Funding acquisition, Resources, Writing - review & editing.

Declaration of Competing Interest

The authors report no declarations of interest.

Acknowledgments

This work was supported by the US Department of Energy's (DOE's) Office of Nuclear Energy under a Nuclear Engineer University Program (award number: DE-NE0008532) and by Westinghouse Electric Company under the DOE ATF program. We also acknowledge valuable discussions with Dr. Andrew T. Nelson of Oak Ridge National Laboratory on experiment design and data interpretation, including water steam testing and corrosion resistance of the silicide fuels.

Appendix A. Supplementary data

Supplementary material related to this article can be found, in the online version, at doi:<https://doi.org/10.1016/j.corsci.2020.109001>.

References

- [1] T. Imanaka, G. Hayashi, S. Endo, Comparison of the accident process, radioactivity release and ground contamination between Chernobyl and Fukushima-1, *J. Radiat. Res.* 56 (2015) i56–i61.
- [2] E.D. Blandford, J. Ahn, Examining the nuclear accident at Fukushima Daiichi, *Elements* 8 (2012) 189–194.
- [3] J.M. Harp, P.A. Lessing, R.E. Hoggan, Uranium silicide pellet fabrication by powder metallurgy for accident tolerant fuel evaluation and irradiation, *J. Nucl. Mater.* 466 (2015) 728–738.
- [4] R.E. Hoggan, K.R. Tolman, F. Cappia, A.R. Wagner, J.M. Harp, Grain size and phase purity characterization of U3Si2 fuel pellets, *J. Nucl. Mater.* 512 (2018) 199–213.
- [5] A. Mohamad, Y. Ohishi, H. Muta, K. Kurosaki, S. Yamanaka, Thermal and mechanical properties of polycrystalline U3Si2 synthesized by spark plasma sintering, *J. Nucl. Sci. Technol.* 55 (2018) 1141–1150.
- [6] D.A. Lopes, A. Benarosch, S. Middleburgh, K.D. Johnson, Spark plasma sintering and microstructural analysis of pure and Mo doped U3Si2 pellets, *J. Nucl. Mater.* 496 (2017) 234–241.
- [7] B. Gong, T. Yao, C. Lu, P. Xu, E. Lahoda, J. Lian, Consolidation of commercial-size UO₂ fuel pellets using spark plasma sintering and microstructure/microchemical analysis, *MRS Commun.* 8 (2018) 979–987.
- [8] T. Yao, S.M. Scott, G. Xin, B. Gong, J. Lian, Dense nanocrystalline UO_{2+x} fuel pellets synthesized by high pressure spark plasma sintering, *J. Am. Ceram. Soc.* 101 (2018) 1105–1115.
- [9] B. Gong, T. Yao, P. Lei, J. Harp, A.T. Nelson, J. Lian, Spark plasma sintering (SPS) densified U3Si2 pellets: microstructure control and enhanced mechanical and oxidation properties, *J. Alloys Compd.* (2020), 154022.
- [10] B. Gong, T. Yao, P. Lei, L. Cai, K.E. Metzger, E.J. Lahoda, F.A. Boylan, A. Mohamad, J. Harp, A.T. Nelson, J. Lian, U3Si2 and UO₂ composites densified by spark plasma sintering for accident-tolerant fuels, *J. Nucl. Mater.* (2020).
- [11] J.T. White, A.T. Nelson, J.T. Dunwoody, D.D. Byler, D.J. Safarik, K.J. McClellan, Thermophysical properties of U3Si2 to 1773 K, *J. Nucl. Mater.* 464 (2015) 275–280.
- [12] D.J. Antonio, K. Shrestha, J.M. Harp, C.A. Adkins, Y. Zhang, J. Carmack, K. Gofryk, Thermal and transport properties of U3Si2, *J. Nucl. Mater.* 508 (2018) 154–158.
- [13] K.E. Metzger, T.W. Knight, E. Roberts, X. Huang, Determination of mechanical behavior of U3Si2 nuclear fuel by microindentation method, *Prog. Nucl. Energy* 99 (2017) 147–154.
- [14] B. Gong, D. Frazer, T. Yao, P. Hosemann, M. Tonks, J. Lian, Nano-and micro-indentation testing of sintered UO₂ fuel pellets with controlled microstructure and stoichiometry, *J. Nucl. Mater.* 516 (2019) 169–177.
- [15] A.T. Nelson, Stability of U3Si2 Under H₂O/PWR Coolant Conditions, Los Alamos National Lab. (LANL), Los Alamos, NM (United States), 2017.
- [16] E.S. Wood, J.T. White, C.J. Grote, A.T. Nelson, U3Si2 behavior in H₂O: part I, flowing steam and the effect of hydrogen, *J. Nucl. Mater.* 501 (2018) 404–412.
- [17] E.S. Wood, J.T. White, A.T. Nelson, The effect of aluminum additions on the oxidation resistance of U3Si2, *J. Nucl. Mater.* 489 (2017) 84–90.
- [18] E.S. Wood, C. Moczygemba, G. Robles, Z. Acosta, B. Brigham, C.J. Grote, K. Metzger, L. Cai, High temperature steam oxidation dynamics of U3Si2 with alloying additions: Al, Cr, and Y, *J. Nucl. Mater.* (2020), 152072.
- [19] L.H. Ortega, B.J. Blamer, J.A. Evans, S.M. McDeavitt, Development of an accident-tolerant fuel composite from uranium mononitride (UN) and uranium sesquisilicide (U₃Si₂) with increased uranium loading, *J. Nucl. Mater.* 471 (2016) 116–121.
- [20] J.H. Yang, D.-J. Kim, K.S. Kim, Y.-H. Koo, UO₂-UN composites with enhanced uranium density and thermal conductivity, *J. Nucl. Mater.* 465 (2015) 509–515.
- [21] K.D. Johnson, A.M. Raftery, D.A. Lopes, J. Wallenius, Fabrication and microstructural analysis of UN-U3Si2 composites for accident tolerant fuel applications, *J. Nucl. Mater.* 477 (2016) 18–23.
- [22] Z. Huang, J. Xing, C. Guo, Improving fracture toughness and hardness of Fe₂B in high boron white cast iron by chromium addition, *Mater. Des.* 31 (2010) 3084–3089.
- [23] E.S. Wood, J.T. White, C.J. Grote, A.T. Nelson, U3Si2 behavior in H₂O: part I, flowing steam and the effect of hydrogen, *J. Nucl. Mater.* 501 (2018) 404–412.